Diverse anthropogenic disturbances shift Amazon forests along a structural spectrum

Marielle N Smith[1,2*], Scott C Stark[1], Tyeen C Taylor[3], Juliana Schietti[4,5], Danilo Roberti Alves de Almeida[6], Susan Aragón[7], Kelly Torralvo[5], Albertina P Lima[5], Gabriel de Oliveira[8], Rafael Leandro de Assis[5,9], Veronika Leitold[10], Aline Pontes-Lopes[11], Ricardo Scoles[7], Luciana Cristina de Sousa Vieira[12], Angelica Faria Resende[6], Alysha I Coppola[13], Diego Oliveira Brandão[5], João de Athaydes Silva Junior[14], Laura F Lobato[7], Wagner Freitas[7], Daniel Almeida[7], Mendell S Souza[7], David M Minor[10], Juan Camilo Villegas[15], Darin J Law[16], Nathan Gonçalves[1], Daniel Gomes da Rocha[17,18], Marcelino Carneiro Guedes[19], Hélio Tonini[20], Kátia Emídio da Silva[21], Joost van Haren[22,23], Diogo Martins Rosa[5], Dalton Freitas do Valle[5], Carlos Leandro Cordeiro[24], Nicolas Zaslavsky de Lima[7], Gang Shao[1,25], Imma Oliveras Menor[26], Georgina Conti[27], Ana Paula Florentino[5], Lía Montti[28], Luiz EOC Aragão[11], Sean M McMahon[29], Geoffrey G Parker[29], David D Breshears[16,30], Antonio Carlos Lola Da Costa[14], William E Magnusson[5], Rita Mesquita[5], José Luís C Camargo[5], Raimundo C de Oliveira[31], Plinio B de Camargo[32], Scott R Saleska[30], and Bruce Walker Nelson[5]

Amazon forests are being degraded by myriad anthropogenic disturbances, altering ecosystem and climate function. We analyzed the effects of a range of land-use and climate-change disturbances on fine-scale canopy structure using a large database of profiling canopy lidar collected from disturbed and mature Amazon forest plots. At most of the disturbed sites, surveys were conducted 10–30 years after disturbance, with many exhibiting signs of recovery. Structural impacts differed in magnitude more than in character among disturbance types, producing a gradient of impacts. Structural changes were highly coordinated in a manner consistent across disturbance types, indicating commonalities in regeneration pathways. At the most severely affected site – burned *igapó* (seasonally flooded forest) – no signs of canopy regeneration were observed, indicating a sustained alteration of microclimates and consequently greater vulnerability to transitioning to a more open-canopy, savanna-like state. Notably, disturbances rarely shifted forests beyond the natural background of structural variation within mature plots, highlighting the similarities between anthropogenic and natural disturbance regimes, and indicating a degree of resilience among Amazon forests. Studying diverse disturbance types within an integrated analytical framework builds capacity to predict the risk of degradation-driven forest transitions.

Front Ecol Environ 2023; 21(1): 24–32, doi:10.1002/fee.2590

Forests in the Amazon are experiencing unprecedented rates of disturbance from anthropogenic land-use and climate change-related drivers. Degradation – including via selective logging, wildfire, and forest fragmentation – impacts existing forest, often leaving canopy cover but altering internal structure, microclimates, and critical ecosystem services, including biodiversity and carbon storage (Berenguer *et al.* 2014; Barlow *et al.* 2016; Longo *et al.* 2016). Degradation now outpaces deforestation as the major type of anthropogenic disturbance affecting primary forests in the Amazon (Matricardi *et al.* 2020). However, secondary forests naturally regenerating on abandoned agricultural land are also increasing in prevalence in tropical landscapes, and provide an important mechanism of carbon sequestration capable of partially countering large carbon losses from degradation (Poorter *et al.* 2021). Predicting changes to Amazon ecosystem services requires an integrated understanding of forest responses to diverse anthropogenic disturbances and the likelihood of continued degradation versus recovery.

Disturbance alters structural properties of the forest canopy that are tightly linked to function. Forest canopy structure comprises the size, quantity, and spatial arrangement of trees and all aboveground vegetation in a forest. Metrics of canopy structure, such as maximum and mean canopy height, surface rugosity, and gap fraction, are strong predictors of aboveground biomass, biomass dynamics (eg tree growth and death) (Stark *et al.* 2012; Hardiman *et al.* 2013; Almeida *et al.* 2019a), and

[1]*Department of Forestry, Michigan State University, East Lansing, MI;* [2]*School of Natural Sciences, College of Environmental Sciences and Engineering, Bangor University, Bangor, UK* *(marielle.smith@bangor.ac.uk); [3]*Department of Civil and Environmental Engineering, University of Michigan, Ann Arbor, MI;* [4]*Departamento de Biologia, Universidade Federal do Amazonas, Manaus, Brazil;* [5]*Instituto Nacional de Pesquisas da Amazônia, Manaus, Brazil;* [6]*Department of Forest Sciences, "Luiz de Queiroz" College of Agriculture, University of São Paulo, Piracicaba, Brazil;* [7]*Programa de Pós-Graduação em Recursos Naturais da Amazônia, Universidade Federal do Oeste do Pará, Santarém, Brazil;* [8]*Department of Earth Sciences, University of South Alabama, Mobile, AL;* [9]*Natural History Museum, University of Oslo, Oslo, Norway;* [10]*Department of Geographical Sciences, University of Maryland, College Park, MD;* [11]*Divisão de Observação da Terra e Geoinformática, Instituto Nacional de Pesquisas Espaciais, São José dos Campos, Brazil;* [12]*Instituto Nacional de Pesquisas Espaciais, Eusébio, Brazil;* [13]*Geological Institute Biogeosciences, ETH Zurich, Zurich, Switzerland;*

(continued on last page)

exchanges of energy, water, and carbon fluxes between forests and the atmosphere (Stark *et al*. 2020; de Oliveira *et al*. 2021). Degradation often acts to open the forest canopy and reduce canopy complexity, thereby increasing albedo and decreasing net radiation, while altering radiative fluxes to the ground (potentially leading to elevated surface radiation and within-canopy temperatures) and the partitioning of sensible and latent heat (evapotranspiration) (Stark *et al*. 2020; de Oliveira *et al*. 2021). Altered (eg hotter) microenvironments can increase forest vulnerability to future disturbances (eg drought, fire; Brando *et al*. 2014; Aragão *et al*. 2018).

The impacts of disturbance vary widely depending on type, intensity, time since impact, and forest type (eg Longo *et al*. 2016). Structural changes following degradation can be modest (for example, under some logging practices) (Longo *et al*. 2016); in such cases, structural recovery can occur rapidly (eg within 10–30 years after fragmentation or drought) (Almeida *et al*. 2019b; Stark *et al*. 2020). At the other extreme, severe structural degradation can lead to a persistent ecological state change. Forest degradation in concert with fire can induce a transition between alternative stable states, from closed-canopy forest to open-canopy savanna-like ecosystems: a shift termed "savannization" (Silvério *et al*. 2013; Oliveras and Malhi 2016). Understanding the mechanisms and probabilities of different forest structural transitions and state changes is key to resolving uncertainty in Amazon forest response to future climate (Malhi *et al*. 2009).

Research attention has focused on the structural impacts of disturbance intensity but has largely neglected the impact of disturbance type (Atkins *et al*. 2020). Of the studies that have investigated disturbance types, most addressed the structural outcomes of one or two agents (for instance, fragmentation [Almeida *et al*. 2019b] as well as fire and logging [Longo *et al*. 2016; Rappaport *et al*. 2018]; all of these studies utilized lidar data). Few studies have investigated a range of disturbance types within an integrated analytical framework (but see Berenguer *et al*. [2014], who assessed multiple disturbance types in Amazon forests using forest inventories, and Atkins *et al*. [2020], who assessed disturbance types in temperate forests using lidar). Lidar is a powerful tool for investigating diverse disturbances because it permits quantification of multidimensional changes, an important feature of disturbance-induced transformations in forest structure that may aid in differentiating between disturbance types (Fahey *et al*. 2019; Atkins *et al*. 2020).

We quantified the consequences of a range of disturbances relating to land use and climate change for tropical forest canopy structure using fine-scale biophysical information from a newly compiled database of ground-based profiling canopy lidar (PCL) data for Amazonia. Collated from lidar surveys conducted for numerous projects over an 11-year period (2008–2019), this large dataset contains observations representing key disturbance types affecting Amazon forests, namely: fragmentation, fire, drought, logging, and land clearing and subsequent forest regrowth. We analyzed structural degradation against a backdrop of natural structural variation among undisturbed Amazon forests that span a spectrum of canopy openness, from tall closed-canopy forests to highly open savanna. We postulated that the savanna state, as an endmember of canopy openness in natural forests, also represents a final state of severe structural degradation in anthropogenically altered forests. Indeed, the potential savannization of the Amazon represents a critical Earth System question influencing the likelihood of destructive climate-change tipping points (Malhi *et al*. 2009; Steffen *et al*. 2018). Despite being floristically distinct (Veldman and Putz 2011), natural and derived savannas appear structurally similar (Stark *et al*. 2020), which is critical for predicting forest microclimates, ecosystem functioning, and the risk of long-term forest transitions.

We tested the hypothesis (H1a) that the impacts of different disturbance types on forest structure can be distinguished because disturbance agents leave distinct structural signatures (Frolking *et al*. 2009; Fahey *et al*. 2019; Atkins *et al*. 2020). For example, drought tends to cause preferential mortality of large trees (Bennett *et al*. 2015), which should result in reductions in canopy height and upper canopy leaf area, whereas surface fires predominantly affect small trees (at least initially), thereby likely reducing lower canopy leaf area (Barlow and Peres 2008). We also tested whether anthropogenically disturbed forests can be distinguished from the natural background of forest structure across the Amazon.

An alternative hypothesis (H1b) – that different disturbance types will not leave distinct structural signatures but will instead be distinguished by the magnitude of their structural impact – was also evaluated. In this case, we expected to find a high degree of coordination among disturbance impacts (ie structural changes will be consistently correlated across disturbance types).

Methods

Deriving metrics of fine-scale canopy structure from lidar

We compiled a large database of PCL data collected across the Amazon (PCL-Am), comprising ground-based lidar data for 370 plots within 36 sites (see WebPanel 1 for lidar survey methods). We focused on 79 disturbed and 62 mature forest "control" plots at nine locations: Biological Dynamics of Forest Fragments Project (BDFFP), Alter do Chão, Universidade Federal do Amazonas (UFAM), Careiro Castanho, Caxiuanã National Forest Reserve, Tapajós National Forest (TNF) Seca Floresta, TNF K81, TNF K83, and Reserva Ducke (WebFigure 1; WebTables 1 and 2). BDFFP, Caxiuanã, and TNF Seca Floresta are sites of experimental manipulations (BDFFP for fragmentation and the other two for drought).

From the lidar data, we generated fully vertically resolved leaf area density (LAD) profiles and identified a focal set of 11

"single value" metrics that quantify different aspects of forest structure (WebTable 3; WebFigure 2): canopy height and variability (maximum and mean canopy height, canopy surface rugosity, and elevation–relief ratio [ERR]), canopy openness and horizontal heterogeneity (gap fraction and heterogeneity fraction), the quantity and density of vegetation (leaf area index [LAI] and leaf area height volume [LAHV]), and the vertical distribution of leaf area and light environments (leaf area weighted height [LAWH], height of 50% LAI, and height of 50% incident light). We compared sites and treatments based on metrics calculated from 20-m transect sections, an ecologically relevant scale that approximates the length scale of understory impacts of canopy gaps and tree crowns in tropical forests (Nicotra *et al.* 1999).

Analysis design

To equally weight disturbed versus undisturbed forests and control for the influence of forest type, we analyzed 11 "treatment pairs" (WebTable 1). Each pair consisted of a set of disturbed forest plots matched with a set of nearby control plots (undisturbed forest plots of the same forest type representing the associated "pre-disturbance" state). Five disturbance types were included in our 11 treatment pairs: fragmentation, surface fire (in lowland "*terra firme*" [non-seasonally flooded] forests and seasonally flooded "*igapó*" forests), experimental drought, reduced-impact logging, and regrowth following land clearing (including secondary forests dominated by members of the tree genera *Vismia* and *Cecropia*) (see WebTable 2 for details of disturbance histories). We also included a naturally occurring savanna site as an outgroup representative of the extreme structural changes that can occur through savannization. Our database did not allow for even-weighting of samples by Amazon region or disturbance type. In addition, we lacked the necessary information to control for disturbance intensity or time since disturbance (most sites were 10–30 years post-disturbance, although disturbance is ongoing within a few sites; WebTable 2), and instead focused on disturbance impact at the time of the lidar survey. Control forests for fragmentation and the savanna outgroup at Alter do Chão have been somewhat disturbed by drought and anthropogenic factors, potentially leading to underestimations of the structural impacts that have occurred at those sites.

We assessed anthropogenic disturbance impacts against the backdrop of natural structural variation among 229 undisturbed Amazon forest plots from the PCL-Am database using hierarchical clustering on principal components (HCPC with the 11 focal metrics; WebPanel 1). We summarized the magnitude of disturbance impacts among treatment pairs by calculating the mean rank order of the absolute differences between disturbed and control forests for all structural metrics; treatment pairs of the same disturbance type were combined where disturbance impacts were similar (WebFigures 3 and 4). Finally, we conducted bivariate regressions between changes in structural metrics (disturbed minus control forests) across treatment pairs to test for coordination of disturbance induced structural impacts. Outliers were first excluded using the interquartile range method of outlier detection.

Results

The impacts of disturbance on the vertical leaf area profile ranged from moving the distribution of foliage upward (one of 11 treatment profiles), no impact (four of 11), to shifting toward a bottom-heavy distribution (six of 11; Figure 1; WebFigure 3g). Following fire in *igapó*, the average height of a leaf (LAWH, a metric of vertical LAD distribution) did not change significantly, but leaf area was lost at all heights (Figure 1k), representing the most severe disturbance impact to the LAD profile. The burned *igapó* profile was most similar to that of the savanna outgroup, although the savanna differed from all disturbed forests in lacking an upper canopy (Figure 1e). Average LAD profiles of disturbed forests differed significantly from undisturbed control forests, with disturbance reducing leaf area in the upper and mid canopy (n = 11 for each type; Figure 1l). Disturbed forests differed significantly from control plots and the wider mature (natural background) forest database for many single-value metrics: mean canopy height, LAWH, LAHV, and heights of 50% LAI and incident light were all lower in disturbed forests, whereas heterogeneity fraction was higher (according to 95% confidence intervals; Figure 2a). Moreover, ERR and LAI were lower in disturbed forests than in mature forest plots (but not paired controls) and gap fraction was higher, while maximum canopy height decreased with respect to control plots (but not mature forests). Notably, structural metrics tended to be more variable among disturbed plots than control plots and the wider mature forest PCL-Am database.

The clustering analysis (HCPC) grouped 72 disturbed plots within clusters that were dominated by mature forest plots (Clusters 2 and 3), and the remainder into a cluster composed of seven disturbed and three mature plots (Cluster 1) (Figure 2b). Many disturbances did not shift the structural composition from one cluster to another. Burned *igapó* exhibited the largest shift, moving from Cluster 2 (mixed) to Cluster 1 (degraded forest-dominated), similar to the differentiation of savanna plots from nearby forest plots at Alter do Chão (Figure 2b).

Drought, fragmentation, and burning of *terra firme* forests led to the smallest structural impacts among our study sites (Figure 3; WebFigures 3 and 4). Forests regenerating after clearcutting and logging displayed medium-level structural impacts, and burned *igapó* exhibited the largest structural differences relative to undisturbed forest. As expected,

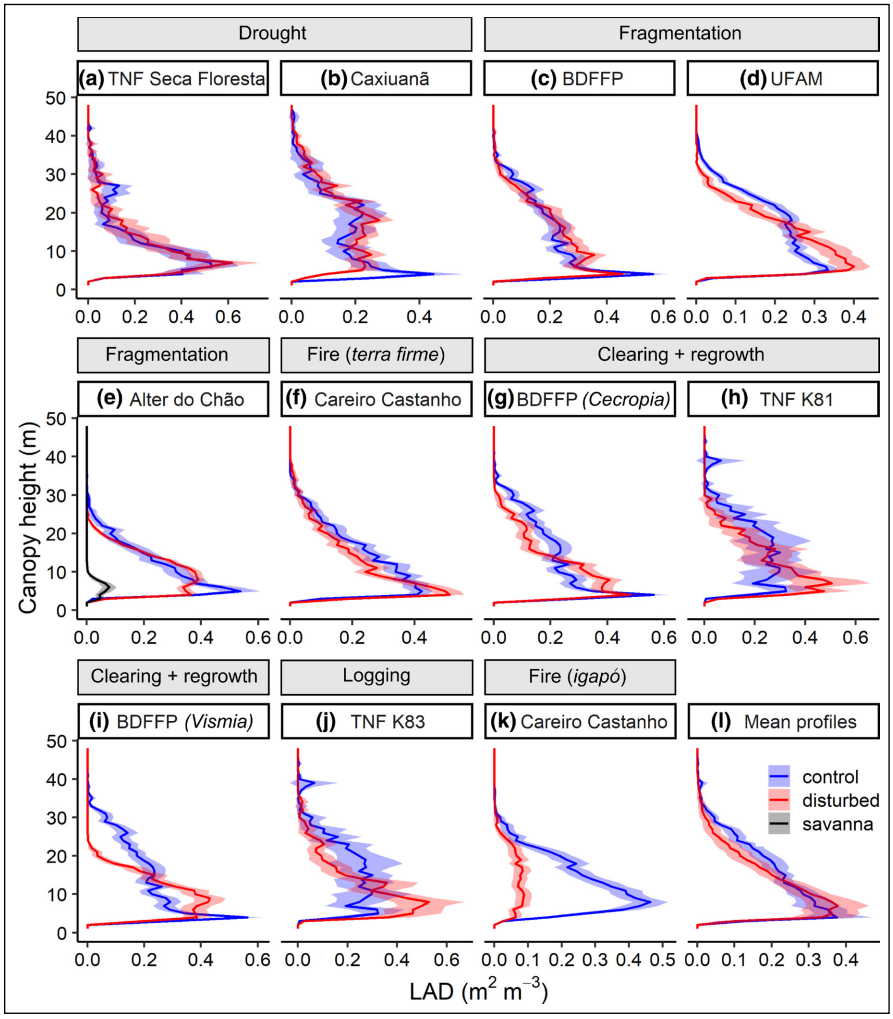

Figure 1. Leaf area density (LAD) profiles for disturbed (red) and undisturbed control (blue) forests for each treatment pair (a–k) and mean LAD profiles of all treatment pairs (l). The LAD profile of a natural savanna site (black), used as an outgroup, is shown in (e). Disturbance types are shown in gray rectangles and plots are ordered by degree of disturbance-induced structural impact, from low (drought) to high (fire in *igapó*). Central lines are means within 95% confidence interval (CI) envelopes.

the savanna site was at the extreme end of structural differences (relative to nearby forest). Structural metrics tended to respond to disturbance in the same direction (increasing or decreasing) across most disturbance types, with the notable exception of surface rugosity (Figure 3). Gap fraction showed very little change, apart from large increases in burned *igapó* and, similarly, gap fraction was higher in the savanna than in nearby forest.

Structural changes induced by disturbance were highly correlated for many metrics (Figure 4; WebFigure 5; WebTable 4). The strongest relationships included changes in canopy height and vertical structure variables (R^2 up to 0.83, $P < 0.0001$). In contrast, metrics of canopy structural heterogeneity exhibited fewer and weaker correlations (ERR and surface rugosity) (R^2 up to 0.52, $P < 0.05$), and in some cases (gap and heterogeneity fractions) no significant correlations were detected. Change in LAI (a metric of leaf quantity) also exhibited only weak correlations (R^2 up to 0.52, $P < 0.05$); notably, however, correlations were higher for change in LAHV (a metric of canopy volume) (R^2 up to 0.83, $P < 0.0001$). For most bivariate relationships, the savanna outgroup and the most highly impacted site, burned *igapó*, were in line with the other treatments, albeit at the extreme ends; however, some metrics (ERR and LAI) identified these sites as outliers.

Discussion

A gradient of structural impacts from anthropogenic disturbances

Overall, forest structural change did not differ in character between disturbance types so much as it differed in magnitude (Figure 3, support for H1b). Most structural metrics changed significantly in response to disturbance and changed in the same direction across disturbance types. Generally, disturbance was associated with a loss of leaf area in the upper canopy, reducing canopy height (mean and maximum) (Figures 1 and 2). Net changes in total leaf area (ie LAI) were small for most disturbances (Figure 3; WebFigure 3), with disturbance instead rearranging the distribution of leaf area, often increasing in the lower canopy (lower LAWH), leading to a reduced height of leaf light interception. In contrast, surface rugosity was highly responsive to disturbance but variable in the direction of change among disturbance types. Two disturbance types did display distinct impacts: secondary forest regeneration ("clearing and regrowth") resulted in a more even-heighted canopy surface (increased ERR), and drought resulted in a more top-heavy leaf area profile (increased LAWH) (Figure 3; WebFigure 3; limited support for H1a); both impacts ran opposite to the trends observed in the other disturbance types, indicating a limited ability to detect certain disturbance agents. Collectively, disturbance and forest types fell along a gradient of structural impacts: from least impact (droughted, fragmented, and burned *terra firme* forests), to more severe impact (secondary and reduced-impact logged forests), and to greatest impact (burned *igapó*) (Figure 3).

The two ends of our gradient of structural impact corresponded to two distinct, intensity-based categories of disturbance described in the literature: (1) non-stand replacing

disturbances with minimal impacts to soil, from which forests can regenerate readily; and (2) disturbances that involve stand-replacement or substantial mortality of canopy trees, as well as severe soil damage, which slows forest recovery (Chazdon 2003; Frolking *et al.* 2009). Drought, fragmentation, and fire in *terra firme* fit within the first category, with low excess mortality rates (~1–5% per year) often differentially affecting large trees (Laurance *et al.* 2006; da Costa *et al.* 2010), although fire impacts are highly variable and can be extreme (Brando *et al.* 2014). Correspondingly, we observed low overall structural impacts and often reduced upper canopy leaf area for these disturbances (Figures 1 and 3; previously documented by Almeida *et al.* 2016, 2019b). We note that our lidar measurements of the Caxiuanã drought experiment did not match this trend, apparently capturing the documented elevated mortality of small- and medium-sized trees (reduced lower canopy leaf area) but not the greater excess mortality of large trees (Figure 1; da Costa *et al.* 2010), perhaps due to our limited sample size. Regrowth following land clearing, reduced-impact logging, and fire in *igapó* forests are examples of the second disturbance category, involving soil degradation and complete (land clearing) or substantial (11–15% of aboveground biomass removed due to logging at TNF K83 [Miller *et al.* 2011]; ~60% loss of trees following fire at the *igapó* site [Resende *et al.* 2014]) removal of forest. Consequently, we observed pronounced reductions in canopy volume (LAHV) and canopy height, and for logged and secondary forests, a significant reorganization of vertical leaf area ~30 years post-disturbance (Figures 1 and 3; WebFigure 3).

Burned *igapó* experienced the greatest structural impacts, including large changes in most metrics, increased canopy openness, and a loss rather than simply a rearrangement of LAI (first reported by Almeida *et al.* 2016). These changes were closely aligned with the savanna outgroup versus mature forest contrast, and consistent with an intermediate forest state that may be at risk of a savanna-state transition (from closed canopy to a persistently open-canopy state; that is, savannization). Seasonally inundated forests are highly vulnerable to savanna-state transitions because

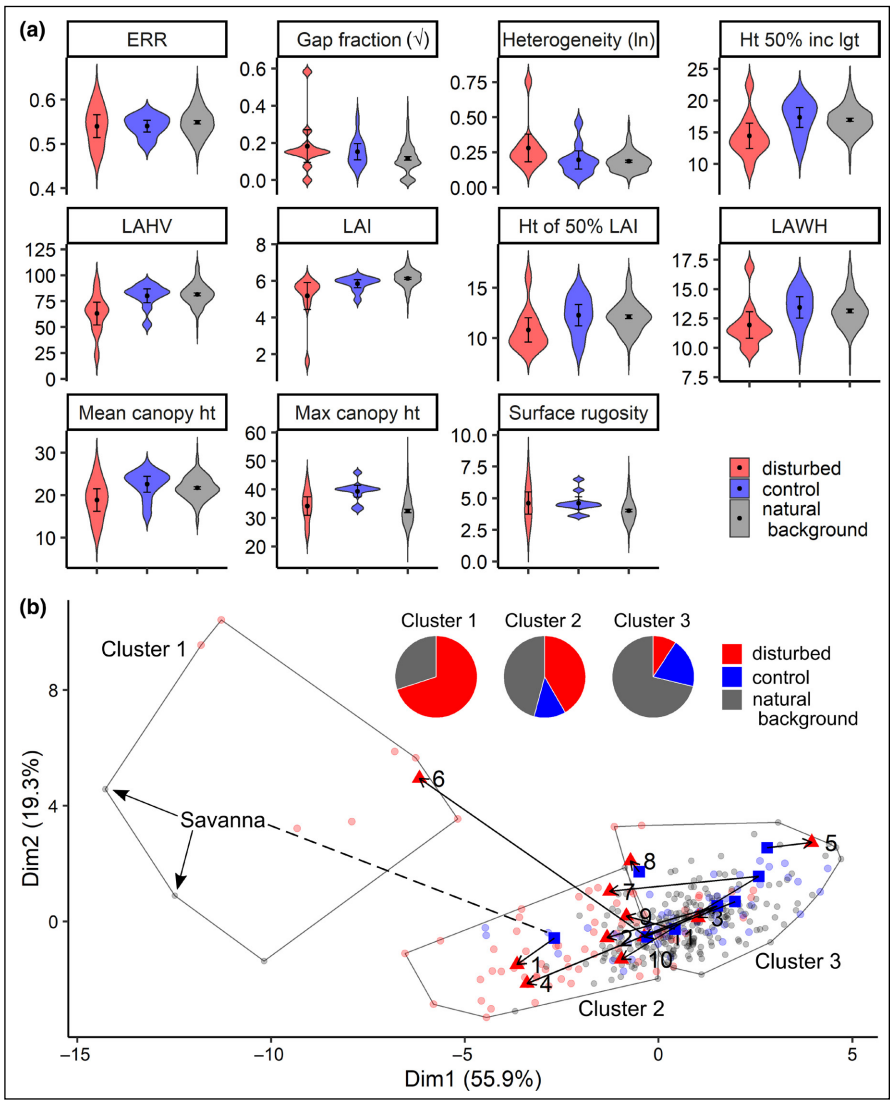

Figure 2. (a) Violin plots displaying the distribution of 11 focal structural metrics within disturbed (red) and control (blue) forests of 11 treatment pairs, and across mature forest plots in the PCL-Am database, used to represent the "natural background" of structural variation (gray, $n = 288$, excludes plots grouped into Cluster 1 in [b]); points and error bars show means and 95% CIs. (b) Output from a hierarchical clustering on principal components analysis (HCPC) applied to the same 11 metrics shown in (a) across all disturbed (red, 79) and control (blue, 62) plots that composed our 11 treatment pairs, in addition to mature forest plots representing the natural background of Amazon forest structure (gray, $n = 229$, from the PCL-Am database). Treatment pairs are represented by blue squares (control forests) and red triangles (disturbed forests), positioned at the central point between survey plots; arrows indicate disturbance-induced structural shifts. Numbers indicate the disturbance treatment pair – 1: fragmentation (Alter do Chão), 2: clearing and regrowth (Biological Dynamics of Forest Fragments Project [BDFFP], *Cecropia*-dominated forest), 3: fragmentation (BDFFP), 4: clearing and regrowth (BDFFP, *Vismia*-dominated forest), 5: drought (Caxiuanã National Forest Reserve), 6: fire (*igapó*), 7: logging (Tapajós National Forest [TNF] K83), 8: drought (TNF Seca Floresta), 9: fire (*terra firme*), 10: clearing and regrowth (TNF K81), and 11: fragmentation (Universidade Federal do Amazonas [UFAM]). The dashed line connects the savanna plots with nearby forest plots. Structural metrics (and units) are as follows: elevation–relief ratio (ERR, unitless), gap fraction (unitless), heterogeneity fraction (unitless), height of 50% incident light (m), leaf area height volume (LAHV, m^3), leaf area index (LAI, $m^2\ m^{-2}$), height of 50% LAI (m), leaf area weighted height (LAWH, m), mean canopy height (m), maximum canopy height (m), and surface rugosity (m).

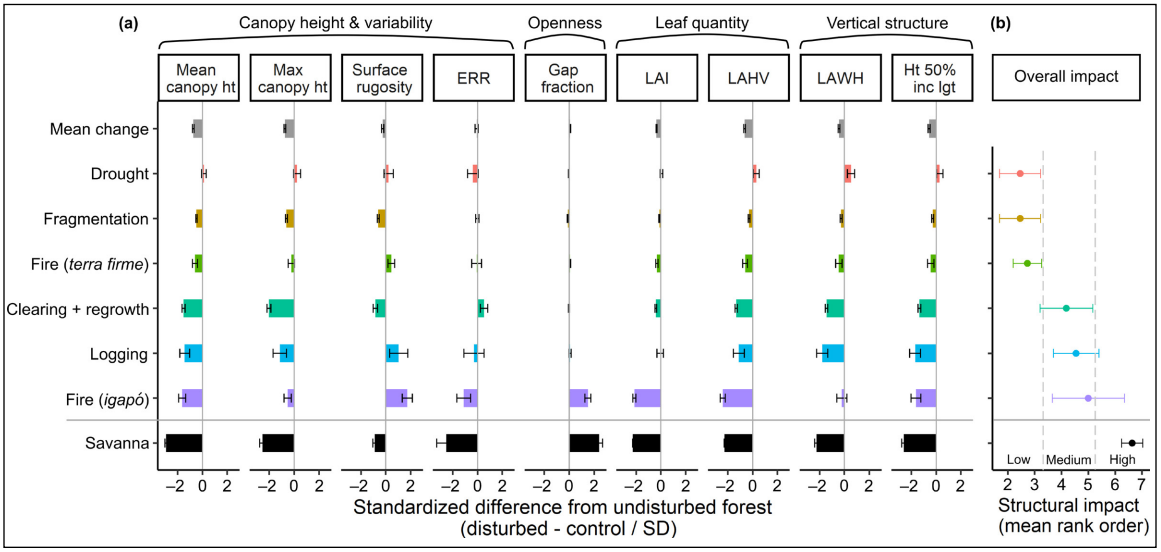

Figure 3. Structural impact of different disturbance types on (a) key structural metrics that are (b) summarized as the mean rank order impact, from least impacted (drought and fragmentation) to most impacted (burned *igapó*), across all 11 focal metrics included in the HCPC. Structural impacts of burned *igapó* closely align with the structural differences between the savanna versus mature forest contrast (outgroup, black). In (a), impact is quantified as the difference in each structural metric relative to the control forest (disturbed minus control), standardized by the standard deviation (SD); bars show means of transect sections and error bars indicate 95% CIs; gray vertical lines at zero indicate no change relative to the control. Disturbance types are separated into forest type where the latter has an important effect (fire in *terra firme* versus *igapó* forests). Structural metrics are as follows: mean canopy height, maximum canopy height, surface rugosity, ERR, gap fraction, LAI, LAHV, LAWH, and height of 50% incident light.

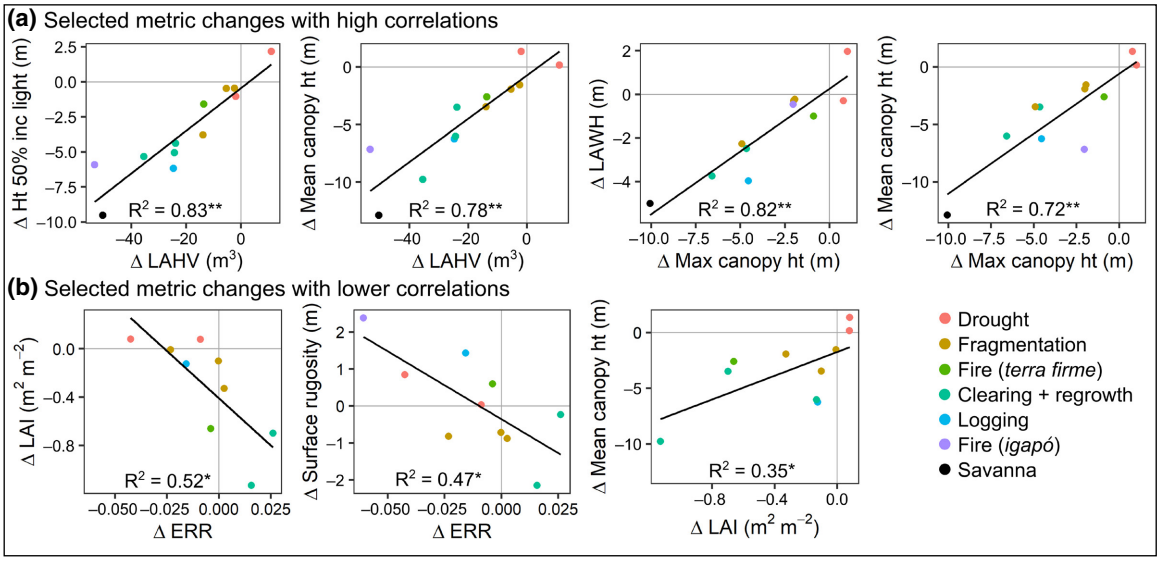

Figure 4. Bivariate relationships between changes in structural metrics (relative to undisturbed control forest mean) across disturbance treatments and savanna outgroup for selected metric changes with (a) high correlations and (b) lower correlations. Gray horizontal and vertical lines indicate no change relative to undisturbed control forests. Regressions exclude points determined as outliers via the interquartile range method of outlier detection. Outliers were as follows – Δ maximum canopy height: BDFFP *Vismia*; Δ ERR: savanna and TNF K81; Δ LAI: savanna and *igapó*. Significance levels: $^{*}P<0.05$, $^{**}P<0.001$.

slow regrowth following fire maintains an open canopy structure and promotes future fire incidence (Almeida *et al.* 2016; Flores *et al.* 2017). Impacts were nearly as severe in logged and secondary forests (Figure 3), yet they did not exhibit canopy opening or large losses in LAI. Instead, lower canopy leaf area increased relative to control forests, consistent with forest recovery that may indicate resilience to disturbance.

Coordination of disturbance-induced structural changes

Overall, we did not observe distinct structural impacts associated with different disturbance agents in our dataset. Rather, structural impacts were aligned along a gradient, and as we predicted, were highly coordinated across disturbance treatments (strong correlations between the

changes in many metrics; Figure 4). The only exceptions were the burned *igapó* and the natural savanna sites, which were consistently at the extreme ends of bivariate relationships, or classed as outliers. In contrast, a similar study by Atkins *et al.* (2020) also using lidar, but in temperate forests, observed distinct signatures of different disturbance types. Disturbance intensity at our sites was possibly too low to leave distinct structural signatures, although this seems unlikely given our observations of significant structural impacts (disturbed versus control plots). Alternatively, the coordinated structural changes that we observed may be a product of forest recovery. Most of our sites were surveyed 10–30 years post-disturbance, and previous studies of two of them documented substantial recovery of forest structure within this timeframe (TNF Seca Floresta drought experiment [Stark *et al.* 2020] and BDFFP forest fragments [Almeida *et al.* 2019b]). All but one of the lidar surveys in Atkins *et al.* (2020) were conducted immediately after disturbance or during ongoing chronic disturbances. We suggest that the disturbance types studied here may have elicited distinct, uncoordinated impacts on canopy structure, but these were relatively transient; subsequently, structural changes became coordinated, indicating fundamental commonalities to structural regeneration trajectories. For example, many of our sites exhibited growth of the lower canopy, a regeneration response (gap infilling) stimulated by elevated light levels following the removal or death of canopy trees (Miller *et al.* 2011; Almeida *et al.* 2019b) that may indicate forest resilience to disturbance.

In contrast, we did not observe a similar recovery response in the fire-affected *igapó*. The persistent lack of canopy regeneration in this system may indicate a sustained alteration of microclimates, which contributes to a tendency to remain in a degraded, savanna-like state (Resende *et al.* 2014; Almeida *et al.* 2016; Flores *et al.* 2017). The spectrum of forest responses that we observed could be interpreted within the theory of alternative stable states, exemplified by forest–savanna transitions (Oliveras and Malhi 2016; Flores *et al.* 2017). This describes how certain ecosystems can exist in alternative states and can shift from one to the other in the presence of a large enough perturbation, relative to the resilience of the ecosystem. We hypothesize that the observation of similar coordination of structural changes among forests indicates a tendency to revert to their original, closed-canopy forest state, whereas sustained discoordination of structural change indicates a potential to remain in a new stable state.

Detection of disturbance-induced structural impacts via lidar

Our results show that lidar can be used to distinguish magnitudes of response to anthropogenic disturbance, and may enable differentiation between forests on recovery pathways and those at risk of continued degradation (Figures 3 and 4). However, we are limited in our ability to generalize about the impacts of specific disturbance types because our database contained only 1–3 examples of each disturbance type, and did not allow us to control for disturbance intensity or time since disturbance. In all but the most severely impacted forests, metrics of vertical structure (but not LAI) were predictive of multiple disturbance effects (Figure 4), indicating the greater capacity of lidar to monitor moderate disturbance relative to optical remote-sensing platforms (eg Moderate Resolution Imaging Spectroradiometer [MODIS]-derived LAI) (Atkins *et al.* 2020). Integrating the analysis of diverse disturbance types and natural forests in a single analytical framework revealed structural similarities between anthropogenically and naturally disturbed forests, at least at sites where some recovery has occurred (Figure 2b, support for H1b; Franklin *et al.* 2002). Their similarity could simplify how disturbance and recovery processes are represented in ecosystem models, although we note that structural similarity does not necessarily imply floristic and functional similarity (Poorter *et al.* 2021). However, anthropogenic disturbances may be better distinguished from natural disturbances based on spatial uniformity and extent, factors not analyzed here but that should be more readily detectable with larger scale (eg satellite-based) remote sensing. Although we were unable to distinguish between anthropogenic disturbance types when structural changes were moderate, it may be possible to identify structural indicators of particular disturbance types through time-series studies that capture pre-, during, and post-disturbance states.

Implications for the future of Amazon forests

Understanding forest structural feedbacks is critical for predicting when degradation can lead to a persistent state change. Loss of upper canopy leaf area and increased light penetration following disturbance likely create more stressful microclimates in the lower canopy (such as higher temperature, increased light, and greater vapor pressure deficit) (Smith *et al.* 2019; Zellweger *et al.* 2020). Particularly in fire-affected *igapó*, these conditions may inhibit tree recruitment and growth directly and also indirectly by facilitating the recurrence of fire or exacerbating drought, providing mechanisms for forest transitions to degraded savanna-like states (Resende *et al.* 2014; Almeida *et al.* 2016; Flores *et al.* 2017). The interactivity of disturbance types means that transition risks can increase nonlinearly, giving rise to potential threshold-like tipping points (Brando *et al.* 2014). In addition, some changes in ecosystem function may exhibit independent nonlinear or threshold-type responses to land-cover changes, which may contribute to forest change feedbacks that must be accounted for in predictive frameworks (Stark *et al.* 2020).

It is promising that many of the forests included in our analysis exhibited signs of recovery 10–30 years after

disturbance, suggesting a degree of resilience in Amazon forests. Among recovering forests, we found that a change in one aspect of forest structure can be predictive of other, multidimensional structural changes, regardless of forest type or original impact. These coordinated structural changes may predict ecosystem function responses such as changing carbon stocks (Almeida *et al*. 2019a). The area of degraded forest in the Amazon is now larger than the area that has been fully deforested (Matricardi *et al*. 2020) and yet carbon emissions from degradation are less well quantified (but see Berenguer *et al*. 2014; Longo *et al*. 2016; Rappaport *et al*. 2018). A better understanding of fine-scale patterns and mechanisms of structural change in degraded forests builds capacity to estimate carbon stocks and emissions of these regions at larger scales via remote sensing (for example, through spaceborne lidar: the Global Ecosystem Dynamics Investigation [GEDI]), assisting in the growing effort to reduce the uncertainty associated with degraded forest emissions and incorporate them into national forest monitoring and policies (Silva Junior *et al*. 2021). An integrated understanding of the structural signatures of disturbance will help to predict the risks of Amazon forest transitions, enhance identification of degradation types (Almeida *et al*. 2019a; Atkins *et al*. 2020), and improve projections of global ecosystem and climate functions.

Acknowledgements

This paper is dedicated to the memory of Marcelo Menin, a valued colleague and friend, who sadly passed away due to the COVID-19 crisis in Brazil prior to preparation of the manuscript. Financial support for this Special Issue was provided by the US National Science Foundation (NSF DEB award 1924942). We gratefully acknowledge M Menin for contributing the Universidade Federal do Amazonas data to this study. This work was primarily supported by NSF DEB grant 1950080 to Michigan State University (MSU), NSF Macrosystems Biology EF-1340604 to MSU, EF-1340624 to the University of Arizona, and NSF PIRE (0730305). Additional support was provided to MNS through a Thomas Lovejoy Fellowship courtesy of the Biological Dynamics of Forest Fragments Project (BDFFP). JS acknowledges funding from Conselho Nacional de Desenvolvimento Científico e Tecnológico (CNPq) PQ-314149/2020-1 and Coordenação de Aperfeiçoamento de Pessoal de Nível Superior – Brasil (CAPES) for supporting the acquisition of a lidar sensor. AP-L, AFR, and DRAA were supported by the São Paulo State Research Foundation (grants 2016/21043-8, 2019/24049-5, and 2018/21338-3). SA was supported by a CNPq PDJ grant (150827/2013-0) and a CAPES-PNPD post-doctoral scholarship. POPA-PELD (Long Term Ecological Monitoring of Western Pará) establishment was supported by the Programa de Pesquisa em Biodiversidade and by the Centro de Estudos Integrados da Biodiversidade Amazônica, Instituto Nacional de Pesquisas da Amazônia (INPA), and CNPq grant (441443/2016-8). KT was supported by Fundação de Amparo à Pesquisa do Amazonas. APL was supported by CNPq Universal Proc (401.120/2016-3) and POPA-PELD. RS was supported by Instituto Chico Mendes de Conservação da Biodiversidade (ICMBio), Programa de Áreas Protegidas da Amazônia, and CNPq-Universal 2016 (426960/2016-5). TCT was supported by NSF 1754163. AIC was supported by the Swiss National Science Foundation Ambizione (grant PZ00P2_185835). SA and RS would like to acknowledge the continued support of CAPES and CNPq for the education and training of students through Masters fellowships at Programa de Pós-graduação em Recursos Naturais da Amazônia–Universidade Federal do Oeste do Pará (PPGRNA-UFOPA). DDB was supported by NSF EF-1340624. This is study 839 of the BDFFP Technical Series.

Data Availability Statement

Data are archived on GitHub (https://github.com/m-n-smith/PCL-Am-disturbance-dataset).

References

Almeida DRA, Nelson BW, Schietti J, *et al*. 2016. Contrasting fire damage and fire susceptibility between seasonally flooded forest and upland forest in the Central Amazon using portable profiling LiDAR. *Remote Sens Environ* **184**: 153–60.

Almeida DRA, Stark SC, Chazdon R, *et al*. 2019a. The effectiveness of lidar remote sensing for monitoring forest cover attributes and landscape restoration. *Forest Ecol Manag* **438**: 34–43.

Almeida DRA, Stark SC, Schietti J, *et al*. 2019b. Persistent effects of fragmentation on tropical rainforest canopy structure after 20 yr of isolation. *Ecol Appl* **29**: e01952.

Aragão LEOC, Luiz EO, Anderson LO, *et al*. 2018. 21st century drought-related fires counteract the decline of Amazon deforestation carbon emissions. *Nat Commun* **9**: 536.

Atkins JW, Bond-Lamberty B, Fahey RT, *et al*. 2020. Application of multidimensional structural characterization to detect and describe moderate forest disturbance. *Ecosphere* **11**: e03156.

Barlow J and Peres CA. 2008. Fire-mediated dieback and compositional cascade in an Amazonian forest. *Philos T Roy Soc B* **363**: 1787–94.

Barlow J, Lennox GD, Ferreira J, *et al*. 2016. Anthropogenic disturbance in tropical forests can double biodiversity loss from deforestation. *Nature* **535**: 144–47.

Bennett AC, McDowell NG, Allen CD, and Anderson-Teixeira KJ. 2015. Larger trees suffer most during drought in forests worldwide. *Nat Plants* **1**: 15139.

Berenguer E, Ferreira J, Gardner TA, *et al*. 2014. A large-scale field assessment of carbon stocks in human-modified tropical forests. *Glob Change Biol* **20**: 3713–26.

Brando PM, Balch JK, Nepstad DC, *et al*. 2014. Abrupt increases in Amazonian tree mortality due to drought-fire interactions. *P Natl Acad Sci USA* **111**: 6347–52.

Chazdon RL. 2003. Tropical forest recovery: legacies of human impact and natural disturbances. *Perspect Plant Ecol* **6**: 51–71.

da Costa ACL, Galbraith D, Almeida S, *et al*. 2010. Effect of 7 yr of experimental drought on vegetation dynamics and biomass storage of an eastern Amazonian rainforest. *New Phytol* **187**: 579–91.

de Oliveira G, Brunsell NA, Chen JM, *et al*. 2021. Legacy effects following fire on surface energy, water and carbon fluxes in mature Amazonian forests. *J Geophys Res-Biogeo* **126**: e2020JG005833.

Fahey RT, Atkins JW, Gough CM, *et al*. 2019. Defining a spectrum of integrative trait-based vegetation canopy structural types. *Ecol Lett* **22**: 2049–59.

Flores BM, Holmgren M, Xu C, *et al*. 2017. Floodplains as an Achilles' heel of Amazonian forest resilience. *P Natl Acad Sci USA* **114**: 4442–46.

Franklin JF, Spies TA, Van Pelt R, *et al*. 2002. Disturbances and structural development of natural forest ecosystems with silvicultural implications, using Douglas-fir forests as an example. *Forest Ecol Manag* **155**: 399–423.

Frolking S, Palace MW, Clark DB, *et al*. 2009. Forest disturbance and recovery: a general review in the context of spaceborne remote sensing of impacts on aboveground biomass and canopy structure. *J Geophys Res* **114**: G00E02.

Hardiman BS, Gough CM, Halperin A, *et al*. 2013. Maintaining high rates of carbon storage in old forests: a mechanism linking canopy structure to forest function. *Forest Ecol Manag* **298**: 111–19.

Laurance WF, Nascimento HEM, Laurance SG, *et al*. 2006. Rain forest fragmentation and the proliferation of successional trees. *Ecology* **87**: 469–82.

Longo M, Keller M, dos-Santos MN, *et al*. 2016. Aboveground biomass variability across intact and degraded forests in the Brazilian Amazon. *Global Biogeochem Cy* **30**: 1639–60.

Malhi Y, Aragão LEOC, Galbraith D, *et al*. 2009. Exploring the likelihood and mechanism of a climate-change-induced dieback of the Amazon rainforest. *P Natl Acad Sci USA* **106**: 20610–15.

Matricardi EAT, Skole DL, Costa OB, *et al*. 2020. Long-term forest degradation surpasses deforestation in the Brazilian Amazon. *Science* **369**: 1378–82.

Miller SD, Goulden ML, Hutyra LR, *et al*. 2011. Reduced impact logging minimally alters tropical rainforest carbon and energy exchange. *P Natl Acad Sci USA* **108**: 19431–35.

Nicotra AB, Chazdon RL, and Iriarte SVB. 1999. Spatial heterogeneity of light and woody seedling regeneration in tropical wet forests. *Ecology* **80**: 1908–26.

Oliveras I and Malhi Y. 2016. Many shades of green: the dynamic tropical forest–savannah transition zones. *Philos T Roy Soc B* **371**: 20150308.

Poorter L, Craven D, Jakovac CC, *et al*. 2021. Multidimensional tropical forest recovery. *Science* **374**: 1370–76.

Rappaport DI, Morton DC, Longo M, *et al*. 2018. Quantifying long-term changes in carbon stocks and forest structure from Amazon forest degradation. *Environ Res Lett* **13**: 065013.

Resende AF, Nelson BW, Flores BM, and de Almeida DR. 2014. Fire damage in seasonally flooded and upland forests of the central Amazon. *Biotropica* **46**: 643–46.

Silva Junior CH, Carvalho NS, Pessôa A, *et al*. 2021. Amazonian forest degradation must be incorporated into the COP26 agenda. *Nat Geosci* **14**: 634–35.

Silvério DV, Brando PM, Balch JK, *et al*. 2013. Testing the Amazon savannization hypothesis: fire effects on invasion of a neotropical forest by native cerrado and exotic pasture grasses. *Philos T Roy Soc B* **368**: 20120427.

Smith MN, Stark SC, Taylor TC, *et al*. 2019. Seasonal and drought-related changes in leaf area profiles depend on height and light environment in an Amazon forest. *New Phytol* **222**: 1284–97.

Stark SC, Breshears DD, Aragón S, *et al*. 2020. Reframing tropical savannization: linking changes in canopy structure to energy balance alterations that impact climate. *Ecosphere* **11**: e03231.

Stark SC, Leitold V, Wu JL, *et al*. 2012. Amazon forest carbon dynamics predicted by profiles of canopy leaf area and light environment. *Ecol Lett* **15**: 1406–14.

Steffen W, Rockström J, Richardson K, *et al*. 2018. Trajectories of the Earth System in the Anthropocene. *P Natl Acad Sci USA* **115**: 8252–59.

Veldman JW and Putz FE. 2011. Grass-dominated vegetation, not species-diverse natural savanna, replaces degraded tropical forests on the southern edge of the Amazon Basin. *Biol Conserv* **144**: 1419–29.

Zellweger F, De Frenne P, Lenoir J, *et al*. 2020. Forest microclimate dynamics drive plant responses to warming. *Science* **368**: 772–75.

Supporting Information

Additional, web-only material may be found in the online version of this article at http://onlinelibrary.wiley.com/doi/10.1002/fee.2590/suppinfo

[14]Instituto de Geociências, Faculdade de Meteorologia, Universidade Federal do Pará, Belém, Brazil; [15]Grupo de Investigación en Ecología Aplicada, Facultad de Ingeniería, Universidad de Antioquia, Medellín, Colombia; [16]School of Natural Resources and the Environment, University of Arizona, Tucson, AZ; [17]Department of Wildlife, Fish, and Conservation Biology, Graduate Group in Ecology, University of California–Davis, Davis, CA; [18]Grupo de Ecologia e Conservação de Felinos na Amazônia, Instituto de Desenvolvimento Sustentável Mamirauá, Tefé, Brazil; [19]Embrapa Amapá, Macapá, Brazil; [20]Embrapa Pecuária Sul, Bagé, Brazil; [21]Embrapa Amazônia Ocidental, Manaus, Brazil; [22]Biosphere 2, University of Arizona, Tucson, AZ; [23]Honors College, University of Arizona, Tucson, AZ; [24]Instituto Internacional para Sustentabilidade, Rio de Janeiro, Brazil; [25]Purdue University Libraries and School of Information Studies, West Lafayette, IN; [26]Environmental Change Institute, School of Geography and the Environment, University of Oxford, Oxford, UK; [27]Instituto Multidisciplinario de Biología Vegetal, Universidad Nacional de Córdoba, Córdoba, Argentina; [28]Instituto de Investigaciones Marinas y Costeras, Instituto de Geología de Costas y del Cuaternario, Universidad Nacional de Mar del Plata-CONICET, Mar del Plata, Argentina; [29]Smithsonian Environmental Research Center, Edgewater, MD; [30]Department of Ecology & Evolutionary Biology, University of Arizona, Tucson, AZ; [31]Embrapa Amazônia Oriental, Santarém, Brazil; [32]Laboratório de Ecologia Isotópica, Centro de Energia Nuclear na Agricultura, Universidade de São Paulo, Piracicaba, Brazil